MADRID
inter.noise 2019
June 16 - 19
NOISE CONTROL FOR A BETTER ENVIRONMENT

A parallel integration scheme of eigen solutions for duct acoustic modes

Zhang, Penglin[1]
Huang, Yu[2#]
Yang, Cheng[3]
Institute of Vibration Shock and Noise, School of Mechanical Engineering, Shanghai Jiao Tong University
No. 800 Dongchuan Road, Shanghai, China

ABSTRACT

Acoustic liners are widely applied in the aircraft engines to reduce the emission of noise. It is important to acquire the accurate acoustic modes in the duct. A parallel integration scheme based on the classical Runge-Kutta method is proposed to calculate the eigenvalues of duct acoustic modes with a uniform mean flow and an impedance boundary condition. The scheme solves the left-propagating modes and the right-propagating modes separately by a numerical integration method. The transverse wavenumbers and the axial wavenumbers of different acoustic modes are integrated simultaneously. The scheme can deal with Ingard-Myers boundary condition and other modified boundary conditions without any transcendental hypothesis in duct acoustics. The convected instability of at most two duct modes is detected via the parallel integration scheme, which is also verified by the Briggs–Bers stability criterion. The parallel integration scheme would give full numerical solutions of duct acoustic modes. Comparing with previous results, it provides a better way to determine the stability of duct modes directly.

Keywords: duct acoustics, numerical computation, liner, unstable modes
I-INCE Classification of Subject Number: 26

1. INTRODUCTION

Acoustic liners are widely applied in the aircraft engines to reduce the emission of noise. It is important to acquire the accurate acoustic impedance of a liner based on investigating the sound propagation in the lined ducts. The inverse method [1] based on the analytical models of sound propagation in ducts is usually adopted to compute and optimize the acoustic impedance. The mode-matching method is usually preferred to reconstruct the acoustic pressure field in different segments of the ducts among different analytical models, and the sound modes are obtained by solving the transcendental eigen equations and dispersion relation.

[1] aaronzpl@sjtu.edu.cn
[2] yu_huang@sjtu.edu.cn
[3] cheng.yang@sjtu.edu.cn

A root-finding method is an optional way to find the eigenvalues of each sound mode. Ko [2] employed the Newton-Raphson method and the eigenvalues of a nearly rigid wall were used as the initial values for the iteration, but the author did not discuss the robustness of the method. Alonso and Burdisso [3] solved the eigen equations by minimizing the absolute value of the equations. The authors used the Nelder-Mead simplex method to perform the minimization from very low frequencies with the eigenvalues of the rigid-walled duct used as the initial values for the calculation. The method is applicable to the resonator-type liners which are equivalent to a rigid wall at relatively low frequencies. Eversman [4, 5] proposed a more general technique on the basis of the classical Runge-Kutta method. It transformed the eigenvalue problem into an ordinary differential equation that described the changing rate of eigenvalues as a function of the admittance value. The eigen solutions of a hard-walled duct were used as initial values and the eigenvalue problem would be resolved by an integration method. The transverse wavenumbers were obtained by a classical Runge-Kutta method and the axial wavenumbers were obtained via the dispersion relation. The method is effective in obtaining accurate duct modes when the imaginary part of the admittance is non-positive. However, if the imaginary part of the admittance is positive, it might lead to wrong propagating directions of some special duct modes.

The objective of study is to develop a general numerical scheme to explore the eigen solutions to the transcendental equations of a lined duct with uniform mean flow and the propagating direction of each sound mode. The scheme is named as 'parallel integration scheme' in that the transverse wavenumbers and axial wavenumbers are solved out simultaneously through a classical Runge-Kutta method.

The structure of the paper is as follows: The parallel integration scheme is discussed in Section 2, the integration procedure and numerical results for the eigen solutions of a rectangular duct with one-sided soft wall is presented in Section 3, the propagating direction and stability of different sound modes are disscussed in Section 4, and conclusions are drawn finally.Please, do not insert any page numbers and do not include any headers of foot notes, except in the first page of the manuscript for the e-mail addresses.

2. ANALYTICAL MODEL

Based on the fourth order Runge-Kutta method, the parallel integration scheme solves the Cauchy's initial problem specified as follows:

$$\begin{cases} y\ x, y\ = f\ x, y \\ \quad y\ x_0\ = y_0 \end{cases} . \tag{1}$$

The unknown function $y = y(x)$ can be a scalar or vector in Equation 1. To take the two-dimensional vector function $y(x) = \ y_1(x), y_2(x)\ ^T$ as an example, Equation 1 can be expressed below:

$$\begin{cases} y_1\ x\ = f_1\ x, y_1, y_2 \\ y_2\ x\ = f_2\ x, y_1, y_2 \\ \quad y_1\ x_0\ = y_{10} \\ \quad y_2\ x_0\ = y_{20} \end{cases} . \tag{2}$$

The classical Runge-Kutta method is defined by

$$y_1\ x_{n+1}\ = y_1\ x_n\ + \frac{1}{6}\ k_{11} + 2k_{12} + 2k_{13} + k_{14}\ , \tag{3a}$$

$$y_2\ x_{n+1}\ = y_2\ x_n\ + \frac{1}{6}\ k_{21} + 2k_{22} + 2k_{23} + k_{24}\ , \tag{3b}$$

where

$$x_{n+1} = x_n + h, \tag{4a}$$

$$k_{11} = hf_1(x_n, y_1\ x_n\ , y_2\ x_n\ ), \tag{4b}$$

$$k_{21} = hf_2(x_n, y_1\ x_n\ , y_2\ x_n\ ), \tag{4c}$$

$$k_{12} = hf_1\left(x_n + \frac{h}{2}, y_1\ x_n\ + \frac{k_{11}}{2}, y_2\ x_n\ + \frac{k_{21}}{2}\right), \tag{4d}$$

$$k_{22} = hf_2\left(x_n + \frac{h}{2}, y_1\ x_n\ + \frac{k_{11}}{2}, y_2\ x_n\ + \frac{k_{21}}{2}\right), \tag{4e}$$

$$k_{13} = hf_1\left(x_n + \frac{h}{2}, y_1\ x_n\ + \frac{k_{12}}{2}, y_2\ x_n\ + \frac{k_{22}}{2}\right), \tag{4f}$$

$$k_{23} = hf_2\left(x_n + \frac{h}{2}, y_1\ x_n\ + \frac{k_{12}}{2}, y_2\ x_n\ + \frac{k_{22}}{2}\right), \tag{4g}$$

$$k_{14} = hf_2\ x_n + h, y_1\ x_n\ + k_{13}, y_2\ x_n\ + k_{23}\ , \tag{4h}$$

$$k_{24} = hf_2\ x_n + h, y_1\ x_n\ + k_{13}, y_2\ x_n\ + k_{23}\ , \tag{4i}$$

and the step size h, is carefully picked to be a small positive value.

2.1 2D hard-walled rectangular duct with a uniform mean flow

The 2D infinite long rectangular duct is shown in *Fig. 1* below. The Mach number of the uniform mean flow is M. Both sides of the duct are hard.

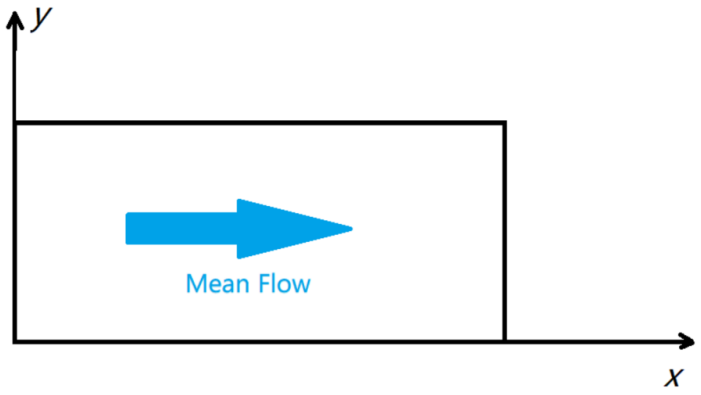

Fig. 1 A 2D infinite long rectangular duct

The sound propagation inside the duct is dominated by the Convected Helmholtz Equation:

$$\frac{\partial^2 p}{\partial x^2} + \frac{\partial^2 p}{\partial y^2} - \left(\mathrm{i}\omega + M\frac{\partial}{\partial x}\right)^2 p = 0. \tag{5}$$

The harmonic solution $e^{\mathrm{i}\omega t}$ represents the real frequency ω. In Equation 5, the dimensionless variables are obtained by the following transformation:

$$x := ax, t := \frac{at}{c_0}, p := \rho_0 c_o^2 p, \rho := \rho_0 \rho, \tag{6a}$$

$$U_\infty := c_0 M, \omega := \frac{\omega c_0}{a}, k := \frac{k}{a}, A := \frac{A}{\rho_0 c_0}. \tag{6b}$$

The hard-walled boundary condition is:

$$\frac{\partial p}{\partial y} = 0, y = 0 \text{ and } y = 1. \tag{7}$$

The general solution of Equation 5 is given by a Fourier modal sum:

$$p = \sum_{m=-\infty}^{+\infty} A_n e^{-\mathrm{i}k_{x,m}x} \; B_m e^{-\mathrm{i}k_{y,m}y} + C_m e^{+\mathrm{i}k_{y,m}y} \quad . \tag{8}$$

Substituting Equation 7 to Equation 8, we have

$$B_m = C_m, k_{y,m} = m\pi, \tag{9}$$

and the dispersion relation

$$k_{x,m}^2 + k_{y,m}^2 = (\omega - M k_{x,m})^2. \tag{10}$$

The axial wavenumber $k_{x,m}$ of the m^{th} mode, $k_{x,m}$, is solved through Equation 10

$$k_{x,m} = \frac{-M\omega \pm \sqrt{\omega^2 - \; 1 - M^2 \; k_{y,m}^2}}{1 - M^2}, \tag{11}$$

and the group velocity is obtained through a deviation of Equation 11

$$c_{g,m} = \frac{\partial \omega}{\partial k_{x,m}} = \left(\frac{\partial k_{x,m}}{\partial \omega}\right)^{-1} = \frac{1 - M^2}{-M \pm \frac{\omega}{\sqrt{\omega^2 - \; 1 - M^2 \; k_{y,m}^2}}}. \tag{12}$$

When $0 \leq k_{y,m} \leq \frac{\omega^2}{1-M^2}$, the axial wavenumbers and the group velocity are real. Since the right-going mode possesses a positive group velocity and the left-going mode possesses a negative group velocity, thus

$$c_{g,+m} = \frac{1 - M^2}{-M + \frac{\omega}{\sqrt{\omega^2 - \; 1 - M^2 \; k_{y,m}^2}}}, \tag{13a}$$

$$c_{g,-m} = \frac{1 - M^2}{-M - \frac{\omega}{\sqrt{\omega^2 - \; 1 - M^2 \; k_{y,m}^2}}}, \tag{13b}$$

then the directions of the two modal solutions of Equation 10 are determined:

$$k_{x,+m} = \frac{-M\omega + \sqrt{\omega^2 - \; 1 - M^2 \; k_{y,m}^2}}{1 - M^2}, \tag{14a}$$

$$k_{x,-m} = \frac{-M\omega - \sqrt{\omega^2 - \; 1 - M^2 \; k_{y,m}^2}}{1 - M^2}. \tag{14b}$$

When $k_{y,m} > \frac{\omega^2}{1-M^2}$, the axial wavenumbers and the group velocity are complex numbers. The amplitudes of the sound modes would not be magnified due to the passive and hard-walled duct, so the exponentially increased solution should be abandoned. Therefore, the axial wavenumber of a right-going mode, $k_{x,+m}$, should possess a positive imaginary part, and the axial wavenumber of a left-going one, $k_{x,-m}$, should possess a negative imaginary part.

Along with Equation 11-14, a new function of the square root is defined in this essay:

$$w := \text{sqrtn } z \;, z \in \mathbb{C}, \text{with}$$

$$\text{sqrtn } z \ = \begin{cases} \sqrt{z}, \text{if } z \text{ is nonegative}, \\ -\text{Sign}(\text{Im}\{\sqrt{z}\})\sqrt{z}, \text{else}. \end{cases} \tag{15}$$

Now the Convected Helmholtz Equation of a 2D-rectangular duct with a uniform flow and two-sided hard walls can be solved completely:

$$p = \sum_{m=-\infty}^{+\infty} A_m e^{-\mathrm{i}k_{x,m}x} \cos(k_{y,m}y)\,, \tag{16}$$

with

$$k_{y,m} = |m|\pi, \tag{17a}$$

$$k_{x,+m} = \frac{-M\omega + \text{sqrtn}[\omega^2 - \ 1 - M^2 \ k_{y,m}^2]}{1 - M^2}, \tag{17b}$$

$$k_{x,-m} = \frac{-M\omega - \text{sqrtn}[\omega^2 - \ 1 - M^2 \ k_{y,m}^2]}{1 - M^2}. \tag{17c}$$

2.2 2D one-soft-walled rectangular duct with a uniform mean flow

The 2D infinite long rectangular duct is presented in *Fig. 2* below. The Mach number of the uniform mean flow is M. A locally-reacting acoustic liner is placed at $y = 1$ and its dimensionless admittance is A.

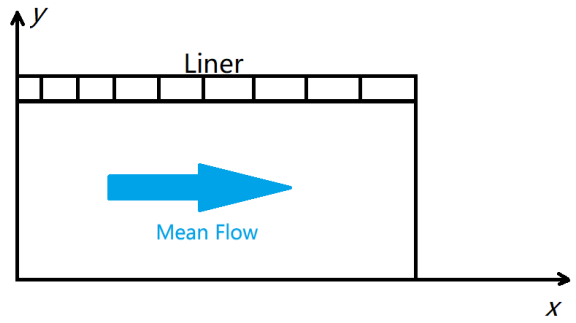

Fig. 2 A 2D rectangular duct with a locally-reacting liner

The boundary condition is:

$$\frac{\partial p}{\partial y} = 0, y = 0, \tag{18a}$$

$$\left(\mathrm{i}\omega + M\frac{\partial}{\partial x}\right)^2 pA = \mathrm{i}\omega\frac{\partial p}{\partial y}, y = 1. \tag{18b}$$

Equation 18b is known as the Ingard-Myers boundary condition.

We have the same result as Equation 16 by substituting Equation 18a to Equation 8. The transcendental eigen equation is obtained below by substituting Equation 16 to Equation 18b

$$\mathrm{i}(\omega - Mk_{x,m})^2 A = \omega\, k_{y,m} \tan k_{y,m}\,. \tag{19}$$

From the above, the transverse wavenumbers and the axial wavenumbers of different sound modes in Equation 16 can be solved along with the dispersion relation in Equation 10.

Equation 19 remains valid for $A = 0$, and it turns out to be the hard-walled boundary condition. If the admittance is slowly changed from $A = 0$ to the target admittance of the acoustic liner in a continuous way, the wavenumber solutions of Equation 10 and 19 would also change continuously from hard-walled solutions to those with liner treatments.

To consider the admittance A as a function of a real parameter η $(0 \le \eta \le 1)$, suppose the admittance of the soft wall is A_w and $A = \eta A_w$, then the wavenumber solutions of

Equation 10 and Equation 19 are depended on η, thus

$$k_{x,m} = k_{x,m}\ \eta\ , k_{y,m} = k_{y,m}\ \eta\ , \tag{20}$$

and they have the initial values at $\eta = 0$ which has been discussed in Section 2.1.

The following ordinary differential equations are obtained by deviating Equation 10 and Equation 19 with respect to η

$$2\mathrm{i}A_w(\omega - Mk_{x,m})\frac{dk_{x,m}}{d\eta} + \omega(k_{y,m}\sec^2 k_{y,m} + \tan k_{y,m})\frac{dk_{y,m}}{d\eta} = \mathrm{i}A_w(\omega - Mk_{x,m})^2, \tag{21a}$$

$$(\omega M + k_{x,m} - M^2 k_{x,m})\frac{dk_{x,m}}{d\eta} + k_{y,m}\frac{dk_{y,m}}{d\eta} = 0. \tag{21b}$$

Thus

$$\frac{dk_{x,m}}{d\eta} = \frac{\mathrm{i}A_w(\omega - Mk_{x,m})^2 k_{y,m}}{2\mathrm{i}A_w(\omega - Mk_{x,m})k_{y,m} - D}, \tag{22a}$$

$$\frac{dk_{y,m}}{d\eta} = \frac{-\mathrm{i}A_w(\omega - Mk_{x,m})^2(\omega M + k_{x,m} - M^2 k_{x,m})}{2\mathrm{i}A_w(\omega - Mk_{x,m})k_{y,m} - D}, \tag{22b}$$

where

$$D = \omega(k_{y,m}\sec^2 k_{y,m} + \tan k_{y,m})(\omega M + k_{x,m} - M^2 k_{x,m}). \tag{22c}$$

To solve for $k_{x,m}$ and $k_{y,m}$ in Equation 22 with the initial values, the classical Runge-Kutta method is applied to calculate the targeted values of eigen solutions of Equation 19.

The hard-walled initial values of transverse wavenumbers should be nonzero to guarantee that Equation 22 is free of singularity. The transverse wavenumber $k_{y,0}$ of a plain wave in a hard-walled duct equals to zero, so this initial value should be replaced by a small positive value. Considering the limit of $k_{y,0}$ when $A \to 0$, from Equation 19, we have

$$k_{y,m} \to \frac{1 \pm M}{1 - M^2}\sqrt{\frac{\mathrm{i}A\Delta\eta}{\omega}}, \tag{23}$$

where $\Delta\eta$ is the initial step away from $\eta = 0$. The recommended value[6] is $\Delta\eta = 0.02$, and we can apply the new initial values of the transverse wavenumber obtained from Equation 23 into the integration scheme to calculate the targeted eigen solutions of the 0^{th} modal solution.

The initial value should be carefully discussed at $\eta = 0$. Substituting $A = \eta A_w$ to Equation 19, we have

$$\eta = \frac{\omega k_{y,m}\tan k_{y,m}}{\mathrm{i}(\omega - Mk_{x,m})^2 A_w}. \tag{24}$$

The normal zeros of the right side in Equation 24 are $0, \pm\pi, \pm 2\pi, \pm 3\pi, \ldots$ which are just the eigen solutions of the duct with two-sided hard walls. They are entitled as 'normal solutions' in this paper. Besides that, Equation 24 may also have asymptotic solutions at infinity. If $M \neq 0, k_{x,m} \to \infty$, we have

$$k_{y,m} = \sqrt{((\omega - Mk_{x,m})^2 - k_{x,m}^2} \to \sqrt{1 - M^2}|k_{x,m}|, \tag{25a}$$

$$\tan k_{y,m} \to \mathrm{i}\,\mathrm{Sign}\left(\mathrm{Im}(k_{y,m})\right), \tag{25b}$$

$$\eta = \frac{\mathrm{i}\omega\sqrt{1 - M^2}}{A_w}\frac{k_{x,m}}{(\omega - Mk_{x,m})^2} \to 0^+. \tag{25c}$$

Since the parameter $\eta \to 0^+$, the imaginary part of A_w should be positive. If so, Equation 25 will have extra asymptotic solutions at infinity (simply entitled as 'extra solutions').

As Equation 25a indicates, we can use a large pure imaginary number as the initial

value of $k_{y,m}$, to solve for the extra solutions. The initial values of two axial wavenumbers are obtained through Equation 17, and then the initial values of η are calculated from Equation 24. The initial parameter η will be complex numbers and the parallel integration scheme cannot be applied directly. Supposing the initial value of η obtained from the previous step is $\eta_0 = s + \mathrm{i}\sigma \ (s > 0)$, the imaginary part of η is changed from σ to 0 with the fixed real part. Thus,

$$\eta = \eta\ \sigma\ = s + \mathrm{i}\sigma, k_{x,m} = k_{x,m}\ \sigma\ , k_{y,m} = k_{y,m}\ \sigma\ , \tag{26}$$

Then

$$\frac{dk_{x,m}}{d\eta} = \frac{dk_{x,m}}{d\sigma}\frac{d\sigma}{d\eta} = \frac{dk_{x,m}}{\mathrm{i}d\sigma}, \tag{27a}$$

$$\frac{dk_{y,m}}{d\eta} = \frac{dk_{y,m}}{d\sigma}\frac{d\sigma}{d\eta} = \frac{dk_{y,m}}{\mathrm{i}d\sigma} \tag{27b}$$

Substituting Equation 27 to Equation 22, $\frac{dk_{x,m}}{d\sigma}$ and $\frac{dk_{y,m}}{d\sigma}$ are solved then. In Step I, the classical Runge-Kutta method is applied to integrate η from $\eta_0 = s + \mathrm{i}\sigma$ to $\eta_1 = s$. The eigenvalues, $k_{x,m}$ and $k_{y,m}$, are also updated to be the new initial values of the next step. In Step II, η is integrated from $\eta_1 = s$ to $\eta = 1$. The wavenumbers during this process are finally changed into the target extra solutions of Equation 19.

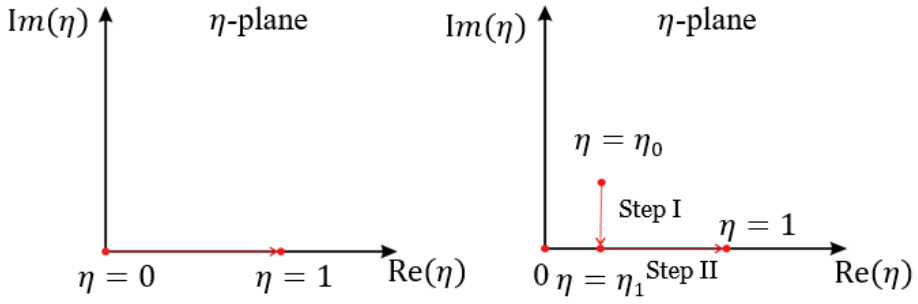

(a) (b)

Fig. 3. The integration path of η (a). for normal solutions; (b). for extra solutions

3. NUMERICAL RESULTS

3.1 Eigen equations without extra solutions at infinity

Usually, the eigen equations only possess normal solutions, thus $M = 0$ or $\mathrm{Im}\{A\} \leq 0$. A case of this condition is studied in this section as an illustration of the proposed integration scheme. As shown in *Fig. 2*, the physical model is a 2D straight duct of infinite length. At $y = 1$, there is a lined wall with an admittance $A = 0.24 - 0.62\mathrm{i}$. The dimensionless frequency ω is 5. Three mean uniform flow conditions are defined by the Mach numbers-$M = 0, M = 0.2$, and $M = 0.4$. The first ten mode solutions of a hard-wall duct is calculated via Equation 17 in *Table 1* below.

Mode	**Transverse wavenumber** $M =$ 0,0.2,0.4	**Axial wavenumber** $M = 0$	$M = 0.2$	$M = 0.4$
1+	0	5.000	4.167	3.571
1-	0	−5.000	−6.250	−8.333
2+	π	3.890	3.063	2.485

2-	π	-3.890	-5.146	-7.247
3+	2π	$-3.805\mathrm{i}$	$-1.042-3.741\mathrm{i}$	$-2.381-3.401\mathrm{i}$
3-	2π	$3.805\mathrm{i}$	$-1.042+3.741\mathrm{i}$	$-2.381+3.401\mathrm{i}$
4+	3π	$-7.989\mathrm{i}$	$-1.042-8.087\mathrm{i}$	$-2.381-8.385\mathrm{i}$
4-	3π	$7.989\mathrm{i}$	$-1.042+8.087\mathrm{i}$	$-2.381+8.385\mathrm{i}$
5+	4π	$-11.53\mathrm{i}$	$-1.042-11.72\mathrm{i}$	$-2.381-12.35\mathrm{i}$
5-	4π	$11.53\mathrm{i}$	$-1.042+11.72\mathrm{i}$	$-2.381+12.35\mathrm{i}$
6+	5π	$-14.89\mathrm{i}$	$-1.042-15.16\mathrm{i}$	$-2.381-16.07\mathrm{i}$
6-	5π	$14.89\mathrm{i}$	$-1.042+15.16\mathrm{i}$	$-2.381+16.07\mathrm{i}$
7+	6π	$-18.17\mathrm{i}$	$-1.042-18.52\mathrm{i}$	$-2.381-19.69\mathrm{i}$
7-	6π	$18.17\mathrm{i}$	$-1.042+18.52\mathrm{i}$	$-2.381+19.69\mathrm{i}$
8+	7π	$-21.42\mathrm{i}$	$-1.042-21.83\mathrm{i}$	$-2.381-23.24\mathrm{i}$
8-	7π	$21.42\mathrm{i}$	$-1.042+21.83\mathrm{i}$	$-2.381+23.24\mathrm{i}$
9+	8π	$-24.63\mathrm{i}$	$-1.042-25.12\mathrm{i}$	$-2.381-26.77\mathrm{i}$
9-	8π	$24.63\mathrm{i}$	$-1.042+25.12\mathrm{i}$	$-2.381+26.77\mathrm{i}$
10+	9π	$-27.83\mathrm{i}$	$-1.042-28.38\mathrm{i}$	$-2.381-30.27\mathrm{i}$
10-	9π	$27.83\mathrm{i}$	$-1.042+28.38\mathrm{i}$	$-2.381+30.27\mathrm{i}$

Table 1 Transverse wavenumbers and axial numbers of a hard-walled rectangular duct with uniform mean flow ($\omega = 5, M = 0, M = 0.2$, and $M = 0.4$).

The parallel integration scheme is then conducted and the trajectory of eigenvalues when η is integrated from 0 to 1 is shown in *Fig. 3*.

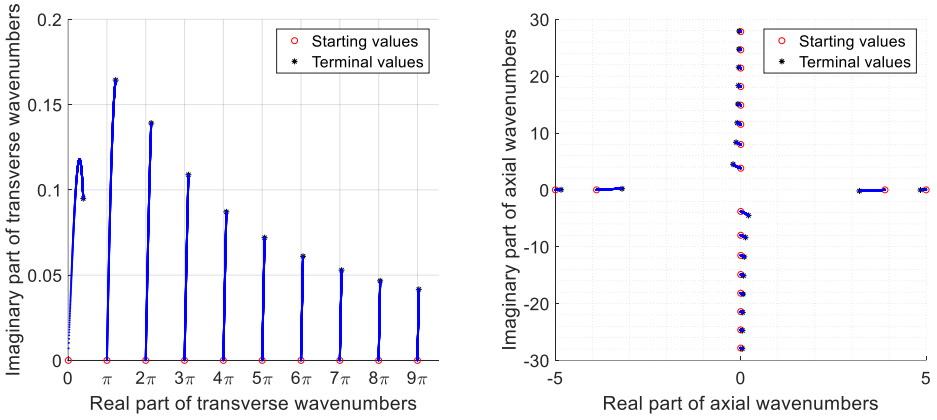

(a)

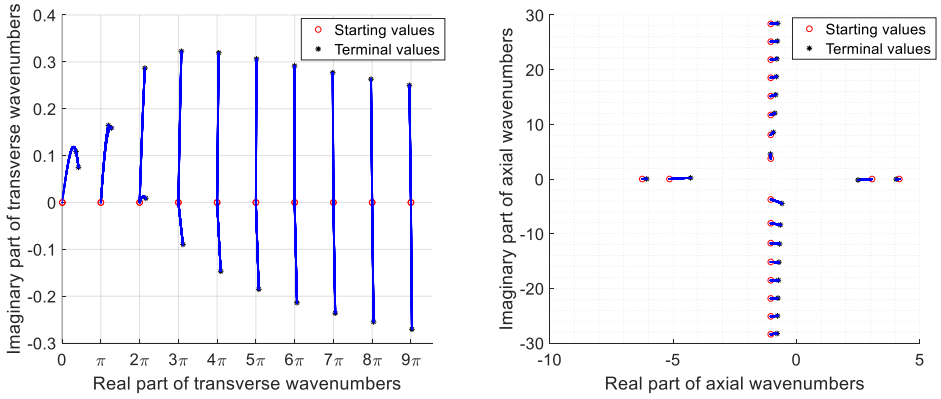

(b)

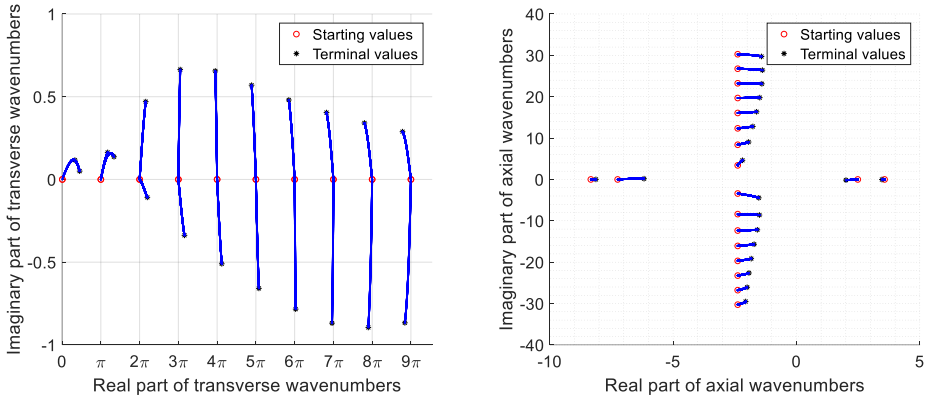

(c)

Fig. 3 Trajectory of eigenvalues when η is integrated from 0 to 1 ($\omega = 5, A = 0.24 - 0.62i$).(a) $M = 0$, (b) $M = 0.2$, (c) $M = 0.4$.

The transverse wavenumbers are selected to have a non-negative real part. The positive resistance assures that the duct is passive, and the axial wavenumbers correspond to this fact. The left-going acoustic modes always possess axial wavenumbers with a positive imaginary part and the right-going acoustic mode possesses axial wavenumbers with a negative imaginary part. The amplitudes of the sound pressure of all duct modes will not be magnified in the duct.

3.2 Eigen equations with extra solutions

According to Section 2.2, the eigen equations will have extra solutions at infinity when the Mach number of the uniform mean flow $M \neq 0$ and the imaginary part of admittance, A, is positive. The same physical model is used here with the only difference that the admittance A is changed to be the conjugate value in Section 3.1, $0.24 + 0.62$i. The first ten mode solutions of a hard-wall duct in Table 1 are still used as initial values of the integration scheme. To calculate the extra eigen solutions, the initial transeverse wavenumber is set to be 100πi, and the initial aixal wavenumbers for right-going and left-going modes are obtained from Equation 17. For normal solutions, the initial value of the integration variable, η_0 is zero and for extra solutions, η_0 is calculated from Equation 23. The trajectory of eigenvalues when η integrated from η_0 to 1 is shown in *Fig. 4*.

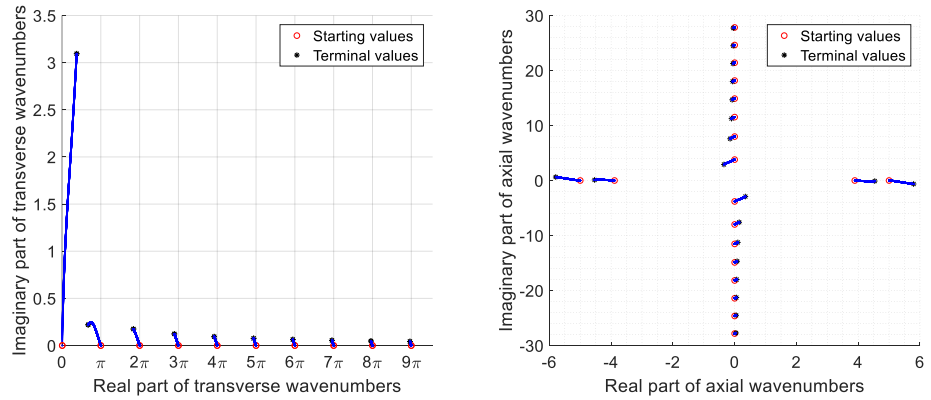

(a)

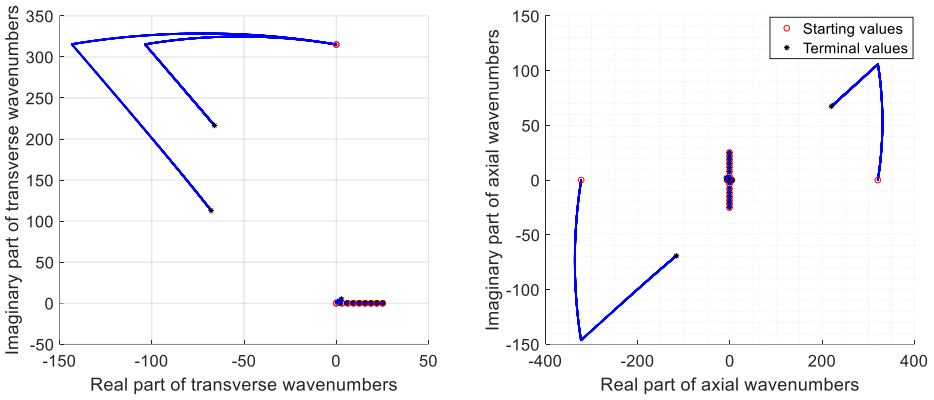

(b)

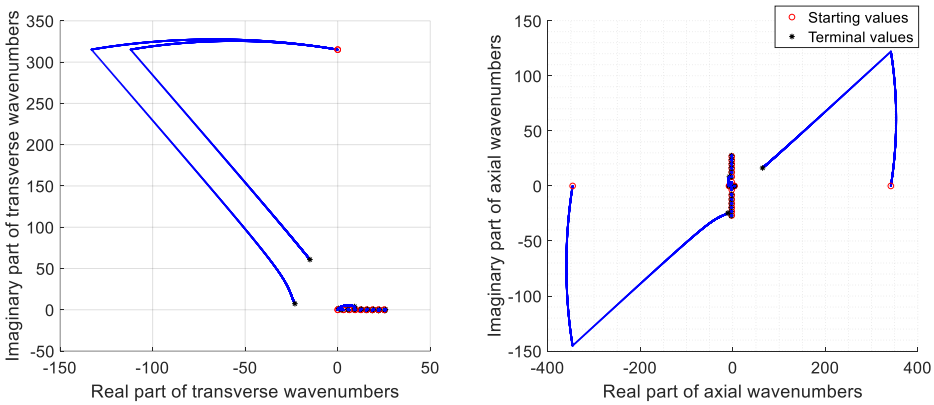

(c)

Fig. 4 Trajectory of eigenvalues when η integrated from η_0 to 1 ($\omega = 5, A = 0.24 + 0.62i$).(a) $M = 0$, (b) $M = 0.2$, (c) $M = 0.4$.

The trajectory of extra wavenumbers in *Fig. 4(b) 4(c)* is quite different from normal ones. The duct modes with these wavenumbers are much more sensitive to the boundary admittance than normal duct modes. Surprisingly, the left-going extra acoustic mode has an axial wavenumber with a negative imaginary part, whereas the right-going extra acoustic mode has an axial wavenumber with a positive imaginary part. It implies that the amplitudes of sound pressure of the two duct modes have been magnified during the propagation in the duct.

4. Discussion

Schmid and Henningson[7] found that an unstable hydrodynamic mode in the duct can occur under certain conditions, which is known as the Kelvin–Helmholtz instability. To verify that the two extra solutions in Section **3.2** are indeed unstable duct modes, the Briggs-Bers causality criteria[8, 9] is applied. The causality confirms that in the duct mode $\mathrm{e}^{\mathrm{i}\,\omega t - kx}$, the axial wavenumber, k, of a right-going acoustic mode locates in the lower complex plane and that of a left-going one locates in the upper complex plane when $\mathrm{Im}\ \omega \ \to -\infty$. The Briggs-Bers criteria states that if the the axial wavenumber of the duct mode crosses the real axis while $\mathrm{Im}\ \omega$ ranges from $-\infty$ to 0, this mode will be convectively unstable. The axial wavenumbers of the first 12 ordinary duct modes and 2 extra duct modes are plotted in *Fig. 5*. In *Fig.5(a)*, the complex frequency ω changes from $5 - 5\mathrm{i}$ to 5 with a increment size of $0.1\mathrm{i}$, and in *Fig. 5(b)*, the complex frequency ω changes from $5 - 15\mathrm{i}$ to 5 with a $0.5\mathrm{i}$ increment. It is demonstrated that the ordinary duct modes are always stable while the 2 extra duct modes are convectively unstable as the

axial wavenumbers cross the real axis when $\mathrm{Im}(\omega)$ changes from a large negative value to 0.

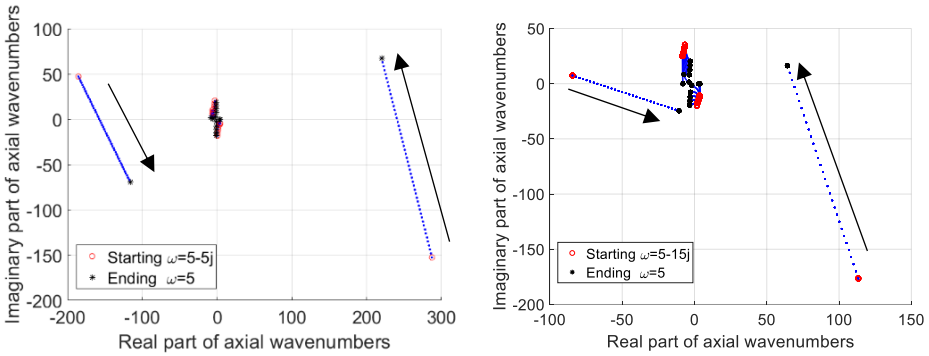

(a) *(b)*

Fig. 5 Trajectory of axial wavenumbers when $Im(\omega)$ changes from a large negative value to 0 $(Re(\omega) = 5, A = 0.24 + 0.62i)$.(a) $M = 0.2$, (b) $M = 0.4$.

The unstable acoustic duct modes act like surface modes discussed by Rienstra [10] and Brambley [11]. The surface modes propagate near the surface of a circular duct and the amplitude of sound pressure decay rapidly in the radial direction. There are at most two hydrodynamic surface modes ("hydrodynamic" means they exist only with flow) propagating in the direction of mean flow in the duct when the Ingard-Myers boundary condition is applied and one of them is convectively unstable. In this paper, the unstable modes also exist only when the flow is present and the imaginary part of the soft wall admittance is positive. Differing from Riensta and Brambley's work, there can be two convectively unstable duct modes propagating in opposite directions in the duct which have been verified by the Briggs-Bers causality criteria in the present study. It might be caused by the different cross-sections of the duct. It might also be attributed to the frequency-independent boundary admittance assumption of this study: the admittance is single-valued at each frequency and the frequency-domain eigen equations are solved by the integration scheme at the given frequency.

5. CONCLUSIONS

This study proposed a parallel integration scheme to obtain the transverse wavenumbers and axial wavenumbers of each duct mode including extra modes. Two convectively unstable duct modes are found in the condition that a mean flow exists in the duct and the admittance of the duct wall possesses a positive imaginary.

The integration scheme is applicable for both forward and inverse problems in the duct acoustics. It can be easily extended to solve the eigen equations of a 3-dimensional duct with other cross-sections. Furthermore, the idea of introducing of new parameters may be useful for the numerical solutions of acoustic modes in a non-uniform duct.

6. REFERENCES

1. Aurégan, Y., M. Leroux, and V. Pagneux, *Measurement of Liner Impedance with Flow by an Inverse Method.* 2013.
2. Ko, S.H., *Sound Attenuation in Lined Rectangular Ducts with Flow and Its Application to the Reduction of Aircraft Engine Noise.* Journal of the Acoustical Society of America, 1971. **50**(6A): p. 1418-1432.
3. Alonso, J.S. and R.A. Burdisso, *Eigenvalue solution for the convected wave equation in a circular soft wall duct.* Journal of Sound & Vibration, 2008. **315**(4): p. 1003-1015.

4. Eversman, W., *Computation of axial and transverse wave numbers for uniform two-dimensional ducts with flow using a numerical integration scheme.* Journal of Sound and Vibration, 1975. **41**(2): p. 252-255.
5. Eversman, W., *Initial values for the integration scheme to compute the eigenvalues for propagation in ducts.* Journal of Sound and Vibration, 1977. **50**(1): p. 159-162.
6. Eversman, W., *Erratum: Computation of axial and transverse wave numbers for uniform two-dimensional ducts with flow using a numerical integration scheme.* Journal of Sound & Vibration, 1976. **47**(1): p. 125-125.
7. Schmid, P.J. and S.H. Dan, *Stability and transition in shear flows* =. 2014.
8. Marcuvitz, N., *Electron-stream interaction with plasmas.* Proceedings of the IEEE, 1964. **53**(11): p. 1808-1809.
9. Bers, A. *Space-time evolution of plasma instabilities—Absolute and convective*. in *Basic Plasma Physics: Selected Chapters, Handbook of Plasma Physics*. 1983.
10. Rienstra, S.W., *A classification of duct modes based on surface waves.* Wave Motion, 2003. **37**(2): p. 119-135.
11. Brambley, E.J. and N. Peake, *Classification of aeroacoustically relevant surface modes in cylindrical lined ducts.* Wave Motion, 2006. **43**(4): p. 301-310.